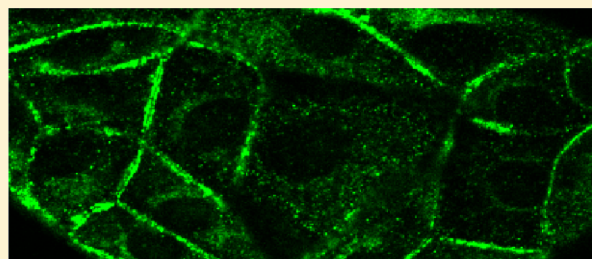


# A Role for G-Proteins in Directing G-Protein-Coupled Receptor–Caveolae Localization

Rhodora Cristina Calizo and Suzanne Scarlata\*

Department of Physiology and Biophysics, Stony Brook University, Stony Brook, New York 11794-8661, United States

**ABSTRACT:** Caveolae are membrane domains that may influence cell signaling by sequestering specific proteins such as G-protein-coupled receptors (GPCRs). While previous reports largely show that  $G\alpha_q$  subunits, but not other G-proteins, interact strongly with the caveolae protein, Caveolin-1 (Cav1), the inclusion of GPCRs in caveolae is controversial. Here, we have used fluorescence methods to determine the effect of caveolae on the physical and functional properties of two GPCRs that have been reported to reside in caveolae, bradykinin receptor type 2 ( $B_2R$ ), which is coupled to  $G\alpha_q$ , and the  $\mu$ -opioid receptor ( $\mu OR$ ), which is coupled to  $G\alpha_i$ . While caveolae do not affect cAMP signals mediated by  $\mu OR$ , they prolong  $Ca^{2+}$  signals mediated by  $B_2R$ . In A10 cells that endogenously express  $B_2R$  and Cav1, downregulation of Cav1 ablates the prolonged recovery seen upon bradykinin stimulation in accord with the idea that the presence of caveolae prolongs  $G\alpha_q$  activation. Immunofluorescence and Förster resonance energy transfer (FRET) studies show that a significant fraction of  $B_2R$  resides at or close to caveolae domains while none or very little  $\mu OR$  resides in caveolae domains. The level of FRET between  $B_2R$  and caveolae is reduced by downregulation of  $G\alpha_q$  or by addition of a peptide that interferes with  $G\alpha_q$ –Caveolin-1 interactions, suggesting that  $G\alpha_q$  promotes localization of  $B_2R$  to caveolae domains. Our results lead to the suggestion that  $G\alpha_q$  can localize its associated receptors to caveolae domains to enhance their signals.



More than 50 years ago, electron micrographs of the plasma membrane of cells revealed dense invaginations of 50–100 nm that were named caveolae (little caves). Caveolae were found to be present in almost all differentiated mammalian cells and are composed of the proteins Caveolin-1 (Cav1) or the muscle specific Caveolin-3 (Cav3), Caveolin-2 (Cav2), and numerous other proteins (see refs 1–3). Many proteins that reside in caveolae are involved in cell signaling, which has led to the speculation that caveolae may be involved in the organization of signaling domains (see refs 4–9). If related signaling proteins localize in caveolae, then these domains could facilitate rapid and directed signals. However, it is unclear whether various signaling proteins localize in caveolae domains because results from immunofluorescence and fractionation studies appear to be contradictory.

An important class of signaling proteins that may target caveolae consists of G-protein-coupled receptors (GPCRs).<sup>10</sup> GPCR signaling occurs through a series of sequential molecular interactions that begin with the binding of an extracellular agonist. This binding is transmitted to downstream effectors in the cytoplasm through activation of heterotrimeric G-proteins.<sup>11</sup> Many GPCRs and G-protein subunits appear to localize to caveolae domains (see refs 10, 12, and 13). Some recent studies of live cells have indicated that components involved in G-protein signaling reside in preformed signaling complexes (e.g., refs 14 and 15) and that Cav1 can alter their interactions by specifically binding to one or more components.<sup>16</sup> Thus, caveolae domains may play a necessary and significant part in GPCR signaling by mediating GPCR

oligomerization, their association with agonists, and their interaction with intracellular G-proteins.

Previous studies have suggested that  $G\alpha_q$  subunits reside in caveolae domains whereas  $G\alpha_o$ ,  $G\alpha_i$ , and  $G\beta\gamma$  subunits prefer non-caveolae domains.<sup>12</sup> Our laboratory used live cell fluorescence imaging and correlation spectroscopy to show that in the basal state  $G\alpha_q$  and  $G\beta\gamma$  localize to caveolae domains.<sup>16</sup> Activation of  $G\alpha_q$  strengthens its interaction with Cav1, promoting the release of  $G\beta\gamma$  subunits from caveolae domains and extending the time of  $G\alpha_q$  activation.<sup>16,17</sup> This stabilization of activated  $G\alpha_q$  through its interaction with Cav1 is seen by a prolonged calcium response that is thought to be due to a combination of stabilization of the activated state of  $G\alpha_q$  by Cav1 and the extended time for  $G\beta\gamma$  recombination. This change in the duration of  $G\alpha_q$ -mediated signals does not appear to be the case for other  $G\alpha$  families.

In this study, we determined whether the presence of caveolae can alter the function and dynamics of two class A GPCRs, the  $\mu$ -opioid receptor ( $\mu OR$ ), which is coupled to  $G\alpha_i$  subunits, and the bradykinin type 2 receptor ( $B_2R$ ), which is coupled to  $G\alpha_q$  subunits. Both receptors have been reported to localize in caveolae (see below). We studied these receptors mainly in Fisher rat thyroid (FRTwt) cells, which do not express detectable levels of Cav1, and a sister cell line that is stably transfected with canine Cav1 (FRTcav+) and displays

Received: August 15, 2012

Revised: October 27, 2012

Published: October 28, 2012

caveolae domains.<sup>18,19</sup> Additionally, FRT cells do not have endogenous  $\mu$ OR or  $B_2R$  receptors, the contribution of which could complicate the analysis of FRET measurements and functional assays.

$\mu$ OR binds morphine and is a target of many analgesics, including opiates (see ref 20).  $\mu$ OR activates  $G\alpha_i$ , resulting in inhibition of adenylate cyclase and a decrease in the level of cellular cAMP. Co-immunoprecipitation studies suggest that  $\mu$ OR localizes to lipid rafts<sup>21,22</sup> and has been shown to localize in Cav3 microdomains in adult cardiomyocytes.<sup>13</sup> Although caveolin expression has not been fully elucidated in the nervous system where  $\mu$ OR is most abundant,<sup>23</sup> it is upregulated in aging brains<sup>24</sup> and its downregulation induces demyelination of neurons.<sup>25</sup> These observations imply that Cav1 may be indirectly involved in promoting changes in plasticity, neuroprotection, neurodegeneration, and aging.

$B_2R$  is a key mediator of the inflammation response.  $B_2R$  signals through  $G\alpha_q$ , resulting in the activation of phospholipase  $C\beta$  (PLC $\beta$ ) resulting in an increase in the level of intracellular calcium and activation of protein kinase C. Unlike  $B_1R$ , which is expressed only during inflammation,  $B_2R$  is expressed continuously, although its tissue expression is limited.<sup>26</sup> We have previously found that in the presence of caveolae, activation of  $G\alpha_q$  by muscarinic receptors results in prolonged calcium responses due to sustained activation of  $G\alpha_q$  by Cav1.<sup>15</sup> Thus, caveolae may promote inflammatory responses through sustained and synergistic  $B_2R$  signaling.

Here, we have used fluorescence methods to study  $\mu$ OR and  $B_2R$ . The use of fluorescence methods allows us to conduct real-time measurements of receptor localization and dynamics in intact cells, thereby eliminating problems associated with cell disruption. We find that the function and localization of  $\mu$ OR are largely unaffected by caveolae. Alternately,  $B_2R$ - $G\alpha_q$  signaling is impacted by caveolae, even though the receptors do not appear to significantly penetrate into these domains. Our FRET studies suggest that receptors do not directly localize to caveolae but require  $G\alpha_q$  to scaffold them to these domains.

## MATERIALS AND METHODS

**Materials.** FRTwt and FRTcav+ cells and canine Caveolin-1-eGFP DNA were gifts from D. Brown (Stony Brook University).  $\mu$ OR-eYFP,  $\mu$ OR-eCFP, and  $G\alpha_i$ -eYFP were from L. Devi (Mount Sinai Medical Center, New York, NY).  $G\alpha_q$ -eYFP and  $G\alpha_q$ -eGFP were from C. Berlot (Geisinger Research).  $B_2R$  and  $B_2R$ -GFP were from F. Leeb-Lundberg (University of Texas Health Science Center). The plasmid of eCFP and eYFP linked by a 12-amino acid peptide chain as a positive control for FRET experiments was from J. Pessin (Albert Einstein College of Medicine, Bronx, NY). mCherry-Cav1, eYFP-Cav1, and eCFP-Cav1 were constructed as described from canine Cav1-eGFP by excising it as a XhoI and BamHI fragment and subcloning it into the same sites in pmcherry-C1, pEYFP-C1, and pECFP-C1 (Clontech). Sequencing of all these plasmids showed an in-frame fusion of mcherry, eYFP, or eCFP at the N-terminus of Cav1 and a six-amino acid linker (SGSRAA) between the Cav1 and fluorophore constructs.

**Cell Culture and Transfection.** FRTwt and FRTcav+ cells have been described previously as were rat aortic smooth muscle cells (A10 cells).<sup>27</sup> Expression of Cav1 in A10 cells was downregulated by treating the cells with siRNA (Cav1) from Dharmacon, Inc., according to the manufacturer's instructions.

The efficiency of downregulation was determined by immunofluorescence using the anti-Cav1 antibody bound to Alexa 647-conjugated secondary antibody in which the fluorescence intensities per cell of wild-type A10 cells ( $n = 11$ ;  $43 \pm 13\%$ ) versus the Cav1 knockdown ( $n = 17$ ;  $21 \pm 7\%$ ) cells were obtained and compared. These measurements showed a Cav1 knockdown efficiency of approximately 51%. Western blot analyses were performed to compare receptor expression levels and were conducted using the reagents and antibodies described in refs 16 and 17.

The levels of expression of Cav1 in FRTcav cells and in transfected HEK293 cells were found to be similar to the endogenous level of expression of Cav1 in NIH3T3, A10, and MDA MB-231 cells by Western blotting. Additionally,  $B_2R$  expression levels in transfected FRT cells were found to be similar to endogenous levels in NIH3T3 cells and A10 cells. Similar expression levels of cells transiently transfected with  $B_2R$  and cells endogenously expressing  $B_2R$  (NIH3T3 and A10 cells) correlate with the comparable extents of calcium release upon stimulation with bradykinin.

**FRET Spectroscopy of Membrane Fractions.** Approximately  $3 \times 10^7$  cells expressing  $B_2R$ -eYFP,  $\mu$ OR-eYFP, or eCFP-Cav1 were homogenized in ice-cold lysis buffer [250 mM sucrose, 20 mM HEPES (pH 7.4), 1.5 mM  $MgCl_2$ , 1 mM EDTA, 1 mM EGTA, protease inhibitor cocktail, 1% Triton X, 0.5% NP-40, and 1 mM DTT]. The membrane fractions were collected by centrifugation at 50000g for 1 h at 4 °C. The concentrations of  $B_2R$ -eYFP and eCFP-Cav1 were found to be 0.12 and 0.30  $\mu$ M, respectively, by Western blot analysis. Expression and purification of recombinant  $G\alpha_q$  and  $G\alpha_i$  through baculovirus infections of Sf9 cells have been described previously.<sup>28</sup>  $G\alpha_q$  and  $G\alpha_i$  were activated by incubation in 1 mM GTP $\gamma$ S in 50 mM HEPES, 100 mM NaCl, 4 mM  $MgCl_2$ , 1 mM DTT, and 50 mM  $(NH_4)_2SO_4$  for 1 h at 30 °C.  $B_2R$ -eYFP (5 nM) and eCFP-Cav1 (10 nM) were titrated with purified  $G\alpha_q$  and  $G\alpha_i$ . FRET measurements between  $B_2R$ -eYFP or  $\mu$ OR-eYFP and eCFP-Cav1 were performed by monitoring the increase in the emission of eYFP (560 nm) upon excitation of eCFP (450 nm) and normalized using the intensities of eYFP emission upon eYFP excitation.

**Ca<sup>2+</sup> Measurements.** Intracellular Ca<sup>2+</sup> levels in cells transiently transfected with  $B_2R$  or  $\mu$ OR were harvested and incubated with 1  $\mu$ M Fura 2-AM in Hanks Balanced Salt Solution (HBSS, Gibco) with 1% BSA. Cells ( $1 \times 10^7$ ) were incubated with 1  $\mu$ M Fura 2-AM for 30 min, pelleted, washed twice with HBSS, and incubated for an additional 15 min for de-esterification of Fura 2-AM. Fluorescence measurements were taken as described in ref 17.

Calcium changes in adherent cells were measured using 5  $\mu$ M Calcium Green, or Calcium Orange if the cells were already expressing a GFP-labeled receptor, on a Zeiss Confocor II instrument as previously described.<sup>17</sup>

**Intracellular cAMP Measurements.**  $\mu$ OR-expressing cells were serum-starved and pretreated with 1 mM 3-isobutyl-1-methylxanthine (IBMX) and stimulated with morphine in the presence of 10  $\mu$ M forskolin. The assay was stopped with 1% perchloric acid and incubated for 1 h. Cyclic AMP was measured from the supernatant using a [<sup>3</sup>H]cAMP assay kit (GE Healthcare) following the manufacturer's instructions. Inhibition of cAMP by morphine is expressed as the percent forskolin activation in the absence of agonist.

**Colocalization Studies.** FRTcav+ cells transfected with  $\mu$ OR-eGFP or  $B_2R$ -eYFP were seeded onto glass bottom dishes

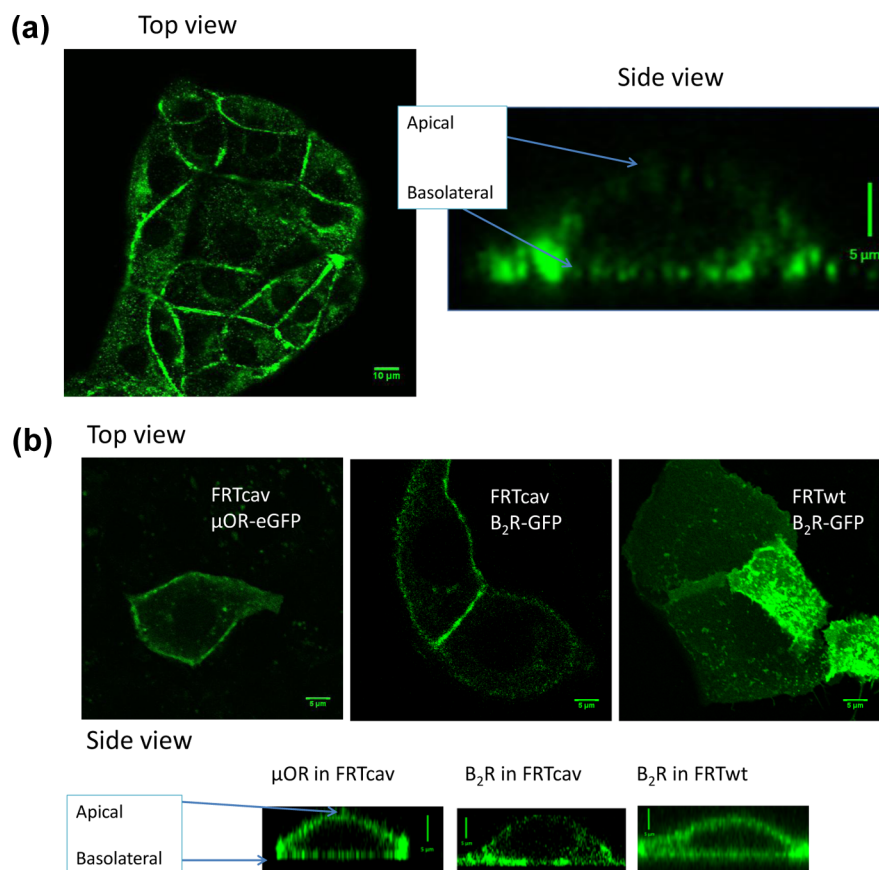


**Figure 1.** (a) Immunofluorescence image of FRTcav+ cells showing the distribution of Cav1 as viewed from the top of the cells. The right panel is a side view of cells showing that Cav1 is mainly distributed on the basolateral region of the plasma membrane. (b) Distribution of  $\mu$ OR and B<sub>2</sub>R in FRT cells.  $\mu$ OR-eGFP in FRTcav+ cells shows a uniform distribution on the apical and basolateral membranes, while the majority of B<sub>2</sub>R-GFP localizes to the basolateral region of FRTcav+ cells, which is similar to the Cav1 distribution. This preferential localization of B<sub>2</sub>R to the basolateral membrane is not seen when it is expressed in FRTwt cells.

(MatTek Corp.). Forty-eight hours post-transfection, cells were washed and fixed with 4% paraformaldehyde for 1 h and permeabilized with 0.2% NP-40. Cells were incubated with rabbit polyclonal anti-Cav1 antibody (N20) (Santa Cruz Biotechnology) and then incubated with AlexaFluor secondary antibodies. Fixed cells were imaged with an Olympus Fluoview laser scanning microscope equipped with a 488 nm argon ion laser for excitation of eGFP, a 534 nm HeNe laser for Alexa 594, or a 633 nm HeNe laser for Alexa 647. No significant bleedthrough was observed from the eGFP or eYFP channel to the Alexa 647 channel. Colocalization analysis was performed using the MacBiophotonics version of ImageJ.

**FRET Imaging.** Sensitized emission FRET was performed with an Olympus Fluoview1000 instrument on HEK293 cells co-expressing eCFP- or eYFP-tagged proteins. eCFP and eYFP were excited using 458 and 515 nm argon ion laser lines, respectively, and 480–495 and 535–565 nm bandpass filters to collect emission images, respectively. The FRET efficiency was calculated by the method used by Chen and co-workers.<sup>29</sup> Using this algorithm, FRET images are corrected for spectral bleedthrough by analyzing images of control cells expressing donor proteins alone or acceptor proteins alone with the same intensity distributions as the sample. Using controls with the same intensity distributions as the samples, we found that FRET efficiency values did not change significantly over a 10-fold range of acceptor:donor intensity ratios (e.g., Figure 5b). Background FRET values were obtained by imaging cells co-

expressing eCFP and eYFP. Positive control values were obtained using a dodecapeptide labeled with eCFP and eYFP on both ends (i.e., eCFP-X<sub>12</sub>-eYFP).

## RESULTS

**Distribution of Caveolae Domains in Cells.** Before characterizing the effect of caveolae on the properties of B<sub>2</sub>R and  $\mu$ OR, we determined the cellular distribution of Cav1 in FRTcav+ cells by immunofluorescence (Figure 1a). FRT cells are polarized epithelial cells that exhibit basolateral and apical membranes. We find that Cav1 is mainly localized to the basolateral membrane and is sporadically distributed on the apical membrane. This is in agreement with the work of Mora and others, who found that more than ~99% of Cav1 in transfected FRT cells preferentially goes to the basolateral membrane.<sup>19</sup> Additionally, Cav1 is localized in regions of cell–cell contact. The observation that Cav1 is concentrated in cell contact regions correlates well with the observation that they may organize proteins involved in intercellular signaling, such as connexins.

We wanted to determine whether the presence of caveolae impacts the plasma membrane distribution of B<sub>2</sub>R and  $\mu$ OR. We looked at the *z* distribution of B<sub>2</sub>R-GFP and  $\mu$ OR-eGFP in FRTcav+ cells to see whether they would have a basolateral distribution similar to that of Cav1. We found that  $\mu$ OR has a uniform plasma membrane distribution on both the basolateral and apical membranes (Figure 1b). Alternately, B<sub>2</sub>R largely

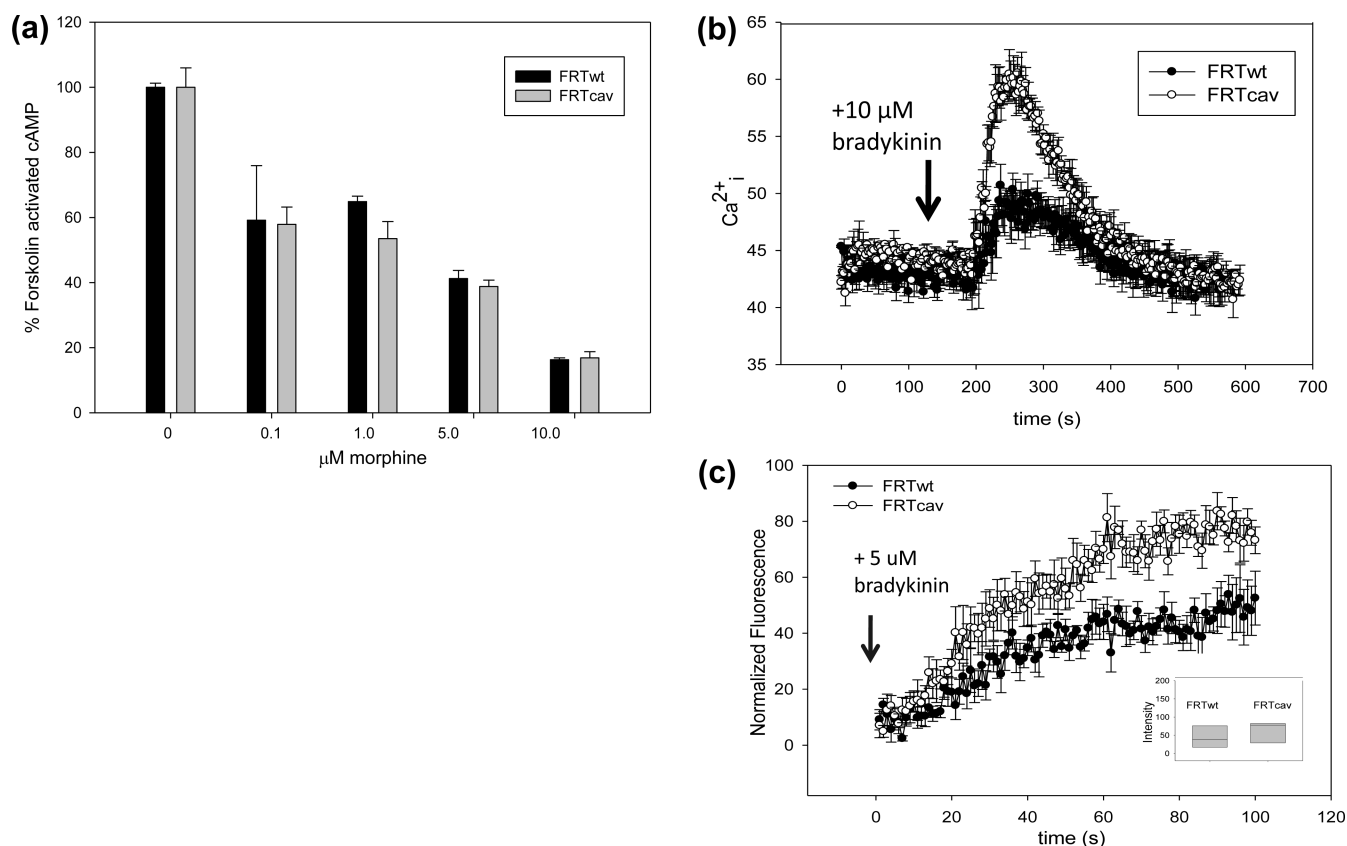


**Figure 2.** (a) Functional studies of suspensions of FRTwt and FRTcav+ cells transfected with  $\mu$ OR, at identical  $\mu$ OR expression levels, showing the differences in cAMP levels stimulated at four different morphine concentrations (see Materials and Methods) where  $n = 3$  independent experiments. The mean  $\pm$  the standard error of the mean (SEM) is shown. (b) Determination of  $\text{Ca}^{2+}$  release in cell suspensions upon the addition of  $10 \mu\text{M}$  bradykinin, as measured using Fura-2, of FRTwt and FRTcav+ cells transfected with  $\text{B}_2\text{R}$  where the expression levels of the receptor were similar in both cell types as determined by Western blot analysis, where  $n = 3$  independent experiments. The mean  $\pm$  SEM is shown. (c) Single-cell measurements of release of  $\text{Ca}^{2+}$  from FRTwt cells transfected with  $\text{B}_2\text{R}$ -GFP and stimulated with  $5 \mu\text{M}$  bradykinin where the curves are an average of responses of eight cells, and the standard deviation is shown. The inset shows the level of  $\text{B}_2\text{R}$ -GFP intensity (y-axis) in arbitrary units of the measured cells.

resides on the basolateral membrane, paralleling the distribution of Cav1 in contrast to  $\mu$ OR. To verify whether the distribution of  $\text{B}_2\text{R}$  is caused by the presence of Cav1, we checked the  $z$  distribution of  $\text{B}_2\text{R}$  in FRTwt cells, which do not have caveolae. In FRTwt cells,  $\text{B}_2\text{R}$  did not exhibit a preferential localization on the basolateral membrane. These observations suggest that Cav1 is responsible for its basolateral localization.

#### Caveolae Affect Signals from $\text{B}_2\text{R}$ but Not from $\mu$ OR.

We determined whether the presence of caveolae alters the ability of  $\mu$ OR and  $\text{B}_2\text{R}$  to generate second messengers. Stimulation of  $\mu$ OR by morphine activates  $\text{G}\alpha_i$ , which inhibits adenylyl cyclase, resulting in a decrease in the level of cellular cAMP. We assessed the decrease in cAMP levels in FRTwt and FRTcav+ cells transfected with  $\mu$ OR using a standard radiometric method (see Materials and Methods). We first verified that the receptor is expressed at similar levels in both cell types by visualizing the fluorescently tagged receptors in live cells. The results of these studies (Figure 2a) demonstrate that caveolae do not affect the cAMP response generated through  $\mu$ OR and  $\text{G}\alpha_i$ . For these cell types, stimulation of  $\mu$ OR and  $\text{G}\alpha_i$  did not increase the level of intracellular  $\text{Ca}^{2+}$  even at saturating morphine concentrations ( $0.1$ – $50 \mu\text{M}$ ).

We have previously found that the affinity between Cav1 and  $\text{G}\alpha_q$  is strengthened when  $\text{G}\alpha_q$  is activated through muscarinic receptors, resulting in a prolonged  $\text{Ca}^{2+}$  signal.<sup>16</sup> Here, we

tested whether a similar increase in the level of calcium is seen for  $\text{B}_2\text{R}$ -mediated  $\text{G}\alpha_q$  activation. To this end, we measured the change in  $\text{Ca}^{2+}$  levels with bradykinin stimulation in FRTwt and FRTcav+ cells expressing  $\text{B}_2\text{R}$ . Again, similar  $\text{B}_2\text{R}$  expression levels in the two cell lines were verified by fluorescence imaging of the tagged receptor (see the inset in Figure 2c). It is notable that the duration of the signal increased  $\sim 2.5$ -fold in the presence of caveolae in addition to the increase in signal magnitude. We determined changes in the  $\text{Ca}^{2+}$  response of single cells (Figure 2c) as well as cell suspensions (Figure 2b). We find that the presence of caveolae significantly increases the amount of  $\text{Ca}^{2+}$  released upon the addition of bradykinin in both calcium assays for cells in suspension ( $t$  test;  $p = 0.007$ ) and single-cell measurements (Mann–Whitney test;  $p = 0.008$ ).

#### Caveolae Affect $\text{B}_2\text{R}$ -Mediated $\text{Ca}^{2+}$ Signaling in A10 Cells.

To support the idea that  $\text{B}_2\text{R}$  signaling can be affected by caveolae in cells that endogenously express both Cav1 and  $\text{B}_2\text{R}$ , we carried out studies using rat aortic smooth muscle cells (A10). In these studies, we compared intracellular  $\text{Ca}^{2+}$  release in wild-type cells and cells where expression of Cav1 was downregulated by  $\sim 50\%$  [as estimated by Western blotting (see Materials and Methods)] through treatment with siRNA(Cav1). In wild-type cells, we find that at least one-third of the cells show a prolonged  $\text{Ca}^{2+}$  signal (i.e.,  $>200$  s) upon bradykinin stimulation that is similar to the behavior

observed for carbachol stimulation of FRTcav+ cell suspensions.<sup>15</sup> In the case of the Cav1 knockdown cells, none of the ~50 siRNA(Cav1) cells showed this prolonged Ca<sup>2+</sup> recovery. In Figure 3, we show data extracted for several cells, although many more were viewed.

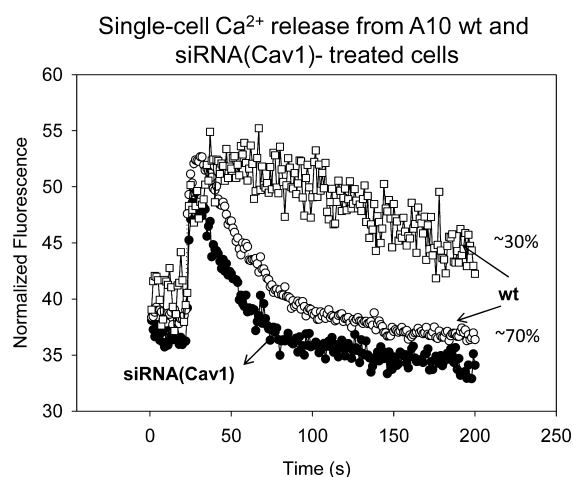


**Figure 3.** Single-cell measurements of Ca<sup>2+</sup>, as determined by Calcium Green (see Materials and Methods) for wild-type A10 cells and cells treated with siRNA(Cav1). Two wild-type traces are shown with empty symbols: (○) average of eight traces for the cell population (~70%) that displayed a short recovery and (□) a sample trace of cells in the 30% population that showed a prolonged recovery (~30%). (●) Average of seven traces for cells that have been treated with siRNA(Cav1). The SEM, which is not shown for the sake of clarity, ranged between 0.6 and 2.5% from the beginning to the recovery period for both types of circles and between 2.4 and 5.7% for the recovery. The error for the prolonged Ca<sup>2+</sup> signal was large in the recovery period and at least 40% higher than that for the short duration cells.

**Colocalization of B<sub>2</sub>R and μOR with Cav1.** The preferential basolateral localization of B<sub>2</sub>R (Figure 1b) and strengthened Ca<sup>2+</sup> signals generated with B<sub>2</sub>R–Gα<sub>q</sub> activation (Figure 2b,c) in FRTcav+ cells suggest that B<sub>2</sub>R, but not μOR, interacts with caveolae domains. As a first step in determining whether this is the case, we measured the amount of colocalization between the receptors and Cav1, using the anti-Cav1 antibody. The results, summarized in Figure 4, show a significant colocalization between B<sub>2</sub>R-eYFP and Cav1 as seen (0.76 ± 0.01; n = 7) on the lateral membrane compared to a positive control consisting of Cav1-eGFP labeled with anti-Cav1 labeled with Alexa 647 in FRTwt cells (0.93 ± 0.01; n = 9) and a negative control consisting of Cav1-eGFP stained with secondary antibody (Alexa 647) alone (0.17 ± 0.02; n = 7). In contrast, a smaller amount of colocalization is seen between μOR-eGFP and Cav1 (0.51 ± 0.01; n = 9).

**B<sub>2</sub>R and μOR Interact Differently with Cav1 As Determined by Förster Resonance Energy Transfer.** Concern with colocalization measurements are the low spatial resolution and the dependence on the strength and specificity of the antibodies, as well as the exposure of the epitope that may be a problem with integral membrane proteins. To gain more sensitive localization information, we used FRET. Cav1 was tagged with an enhanced cyan fluorescent protein (eCFP) on its N-terminus, and B<sub>2</sub>R and μOR were tagged with an enhanced yellow fluorescent protein (eYFP) tag on their C-termini. HEK293 cells were chosen for their high transfection

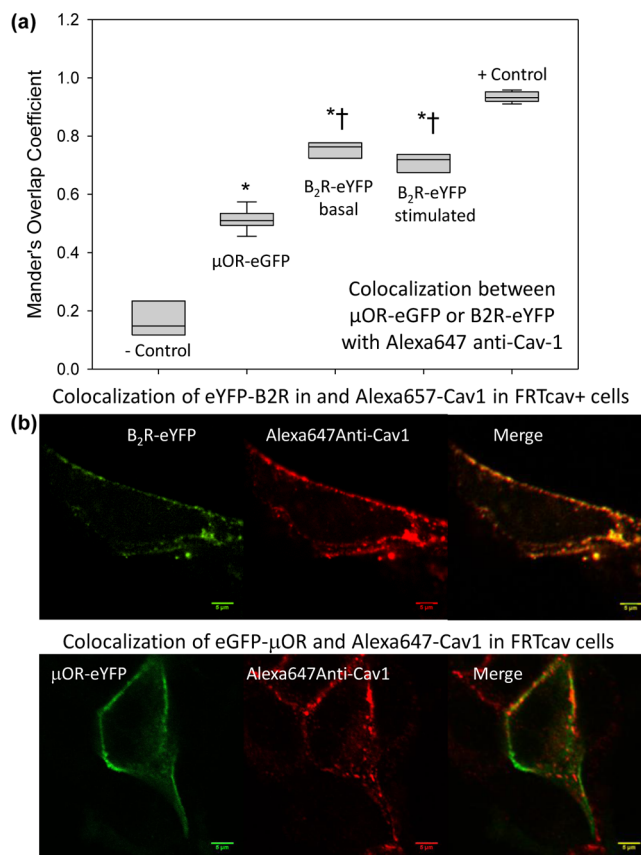


**Figure 4.** (a) Summary of colocalization of Cav1 with μOR and B<sub>2</sub>R as compared to negative and positive controls, where n = 7 for the negative control [Cav1-eGFP and secondary antibody (Alexa 647) alone], n = 9 for μOR-eGFP, n = 7 for unstimulated B<sub>2</sub>R-eYFP, n = 6 for B<sub>2</sub>R-eYFP stimulated with 1 μM bradykinin for 5 min, and n = 9 for the positive control (Cav1-eGFP and Cav1 antibody labeled with the Alexa 647-conjugated secondary antibody). Asterisks indicate significant differences from the negative control, while crosses indicate significant differences from μOR-eGFP–Cav1 colocalization values (ANOVA; p < 0.001). (b) Sample images of some of the cells that were used in the data presented in Figure 3a.

efficiency and the exclusive plasma membrane distribution of the receptors. Moreover, the usage of nonpolarized HEK293 cells removes artifacts that could arise from using FRT cells whose polarity might influence FRET results. Cells expressing eCFP-Cav1 and B<sub>2</sub>R-eYFP at similar levels were selected. The increase in eYFP emission in the presence of eCFP was then measured (see Materials and Methods). For the eCFP/eYFP pair, the distance at which 50% donor fluorescence is lost to transfer is 30 Å, and on the basis of the estimated size of the proteins, the presence of FRET should indicate physical association. FRET values for each sample were compared to a positive control consisting of eCFP-X<sub>12</sub>-eYFP and a negative control consisting of free eCFP and eYFP expressed in the same cells (see refs 14 and 30). Additionally, we verified that a high level of FRET occurs between Cav1-eGFP and mcherry-Cav1, showing that the tagged Cav1 proteins can still oligomerize and form caveolae domains (data not shown). FRET results are summarized in Figure 5. Despite previous data suggesting that μOR localizes in caveolae domains, we could not detect significant FRET between Cav1 and μOR. In contrast, B<sub>2</sub>R and Cav1 display a weak but significant and

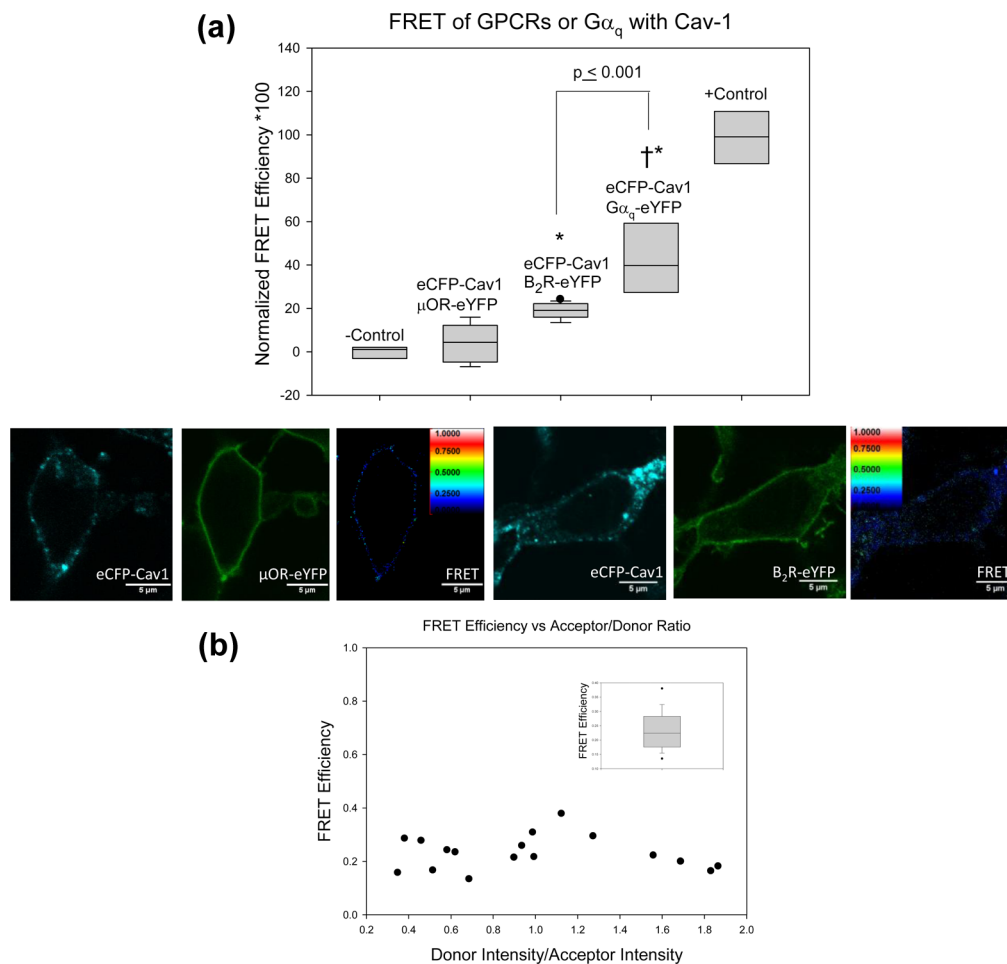


**Figure 5.** (a) Normalized % FRET efficiencies (see Materials and Methods) of eCFP-Cav1 with  $\mu$ OR-eYFP ( $n = 9$ ), eCFP-Cav1 with  $B_2R$ -eYFP ( $n = 15$ ), and eCFP-Cav1 with  $G\alpha_q$ -eYFP ( $n = 7$ ). Asterisks indicate significant differences from the negative control, while a cross indicates a significant difference from values for eCFP-Cav1 with  $B_2R$ -eYFP (ANOVA;  $p < 0.001$ ). Sample raw images of a cell expressing eCFP-Cav1 and  $\mu$ OR-eYFP acceptors and raw FRET (left) and a cell expressing eCFP-Cav1 and  $B_2R$ -eYFP and raw FRET (right). We note that previous studies of eCFP-Cav1 and  $G\alpha_q$ -eYFP expressed in FRTwt cells gave a FRET efficiency of  $4 \pm 6\%$  ( $n = 3$ ). (b) Plot showing that the FRET efficiency between  $B_2R$ -eYFP and eCFP-Cav1 (box plot, inset) does not change significantly over a 10-fold range of donor:acceptor intensity ratios with the FRET algorithm used.

reproducible FRET, suggesting that a population of receptor localizes to these domains.

We find the value of  $G\alpha_q$ -Cav1 FRET is 2-fold higher than the value of  $B_2R$ -Cav1 FRET (Figure 5). Although other interpretations are possible, these results might suggest that  $G\alpha_q$  has a higher degree of caveolae association than  $B_2R$ . We note that the higher level of FRET between  $G\alpha_q$  and Cav1 than between  $B_2R$  and Cav1 is unexpected because we have found a relatively high level of normalized FRET for  $B_2R$ -eYFP and  $G\alpha_q$ -eCFP (i.e.,  $24.7 \pm 1.8$  for FRTwt and  $29.1 \pm 3.3$  for FRTcav+). Moreover, we have previously found that  $B_2R$  forms a complex with  $G\alpha_q G\beta\gamma$  in the basal state of HEK293 cells.<sup>15</sup> Nevertheless, the presence of FRET suggests close localization among  $B_2R$ ,  $G\alpha_q$ , and Cav1.

**Role of  $G\alpha_q$ -Cav1 Interactions in  $B_2R$ -Cav1 Interactions.** Our FRET studies suggest that  $G\alpha_q$ -Cav1 interactions are stronger than  $B_2R$ -Cav1 interactions, and it is possible that  $G\alpha_q$  is responsible for promoting  $B_2R$ -Cav1 interactions. If this is the case, then disrupting  $G\alpha_q$ -Cav1 interactions would eliminate  $B_2R$ -Cav1 FRET. Thus, we measured the amount of FRET between  $B_2R$ -eYFP and eCFP-Cav1 in the absence and presence of a microinjected caveolin peptide (DGIWKASFTTFTVTKYWFYRC), which interferes

with the association between purified  $G\alpha_q$  and partially purified membrane fractions containing overexpressed Cav1.<sup>16</sup> This peptide, but not a control peptide with the same length and charge, also disrupts  $G\alpha_q$ -Cav1 colocalization in cultured cells and cardiomyocytes, although there is a possibility that the peptide might disrupt other Cav1 interactions.

HEK293 cells expressing  $B_2R$ -eYFP and eCFP-Cav1 at similar levels were microinjected with 200 nM peptide, and changes in  $B_2R$ -Cav1 FRET were determined (e.g., Figure 6a). By comparing the amount of FRET from microinjected versus uninjected cells to that in cells injected with 200 nM control peptide, we found that cells injected with caveolin peptide had significantly lower FRET values (Figure 6b). It is worth noting that the FRET values between  $B_2R$ -eYFP and eCFP-Cav1 in microinjected cells were similar to those of negative controls, suggesting that the amount of caveolin peptide microinjected is enough to disrupt the entire population of the  $B_2R$ -eYFP associated with Cav1. This study suggests that the population of  $B_2R$ -eYFP that participates in the transfer of energy from eCFP-Cav1 is mediated by interactions between  $G\alpha_q$  and Cav1.

We further tested this idea by transfecting HEK293 cells with eCFP-Cav1 and  $B_2R$ -eYFP and measuring the decrease in the level of FRET with decreased levels of  $G\alpha_q$  using siRNA-

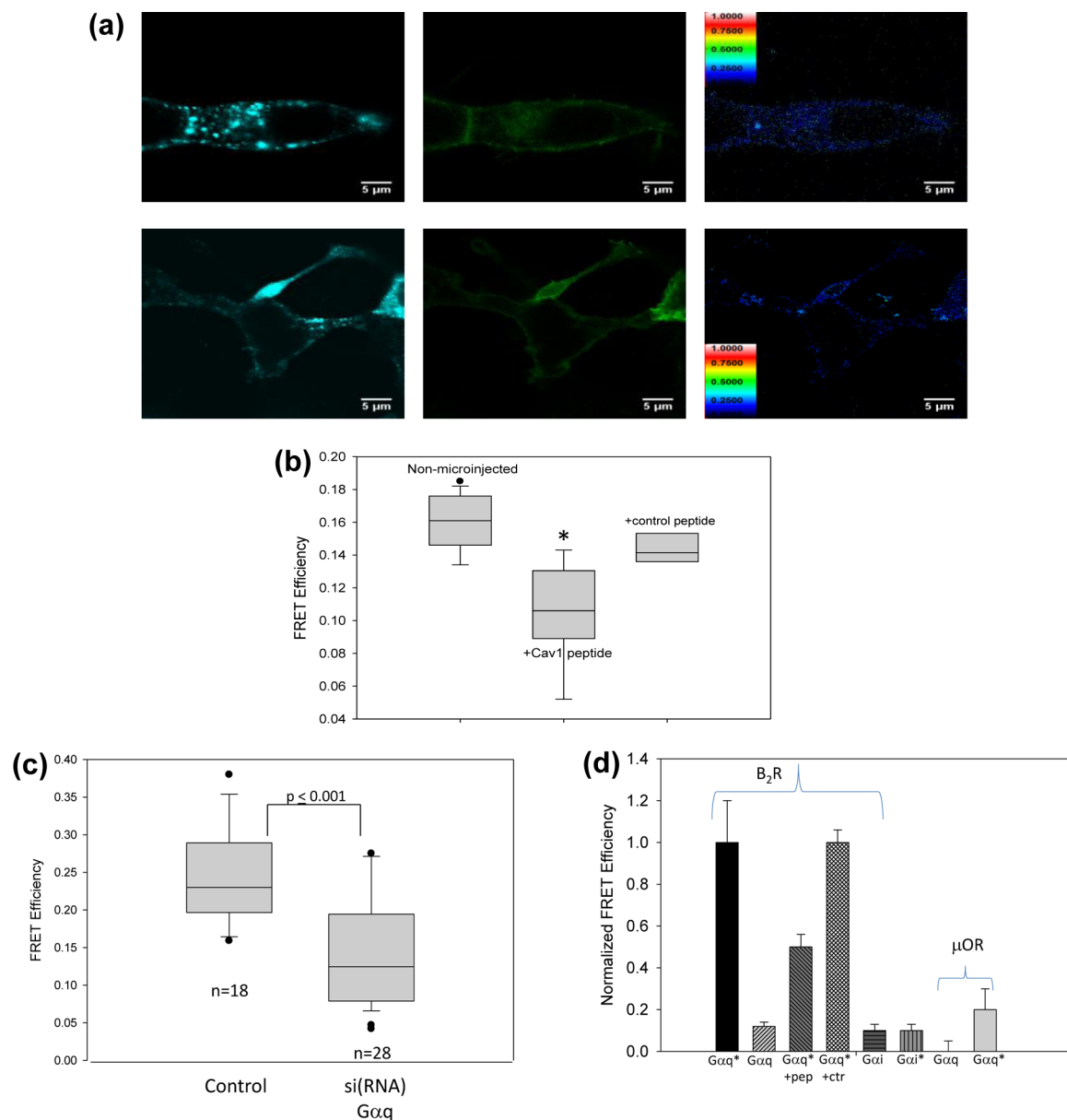


**Figure 6.** (a) Raw images showing the change in FRET between eCFP-Cav1 and B<sub>2</sub>R-eYFP before and after injection with a 200 nM solution of a peptide that disrupts Gα<sub>q</sub>-Cav1 association (Cav1 peptide). We note that the injected cell presented was one that gave a FRET value in the upper range for the purposes of display. (b) Summary of the change in eCFP-Cav1-B<sub>2</sub>R-eYFP FRET in cells that were not injected (*n* = 15), cells injected with the Cav1 peptide (*n* = 9), or a control peptide (*n* = 8). ANOVA calculations show significant differences (*p* < 0.001) between uninjected and Cav1 peptide samples and between Cav1 peptide and control peptide data. (c) Study similar to that shown in Figure 5b except that in this study, Gα<sub>q</sub> was downregulated using siRNA (see the text). (d) FRET between B<sub>2</sub>R-eYFP and eCFP-cav1 in HEK293 membrane fractions mixed with activated (30 nM) (Gα<sub>q</sub><sup>\*</sup> or Gα<sub>i</sub><sup>\*</sup>) or inactivated Gα<sub>q</sub> or Gα<sub>i</sub> (30 nM) in the absence and presence of 200 nM Cav1 peptide (+pep) or 200 nM control peptide (+ctr). FRET efficiencies were calculated from the increase in eYFP emission upon eCFP excitation. Data are means ± SEM, where *n* = 3 independent experiments.

mediated downregulation. Gα<sub>q</sub> was downregulated by  $\sim 39 \pm 11\%$ , as estimated by Western blotting. We note that downregulation of Gα<sub>q</sub> did not affect the expression levels or cellular localization of eCFP-Cav1 and B<sub>2</sub>R-eYFP. Our results (Figure 6c) show that reducing the level of Gα<sub>q</sub> decreases the amount of FRET between B<sub>2</sub>R and Cav1.

To support the hypothesis that Gα<sub>q</sub> is directing B<sub>2</sub>R-Cav1 interactions, we performed spectroscopic FRET of purified membrane fractions from HEK293 cells overexpressing either B<sub>2</sub>R-eYFP or eCFP-Cav1. We then mixed B<sub>2</sub>R-eYFP and eCFP-Cav1 membrane fractions and measured the ability of Gα<sub>q</sub> to promote association. Addition of 30 nM activated Gα<sub>q</sub>

in the absence or presence of a control peptide (see above) resulted in a substantial increase in the level of FRET indicative of B<sub>2</sub>R-Cav1 association (Figure 6d). This increase was reduced in the presence of the caveolin-1 peptide or deactivated Gα<sub>q</sub>(GDP). Addition of activated or deactivated Gα<sub>i</sub> had no measurable effect on the level of FRET. Keeping in mind that the affinity of Gα<sub>q</sub>(GTPγS) for B<sub>2</sub>R is still high under conditions where downregulation does not occur (see ref 15), as is the case here, and that the affinity between Cav1 and activated Gα<sub>q</sub> is very high, this result shows that Gα<sub>q</sub> promotes association between B<sub>2</sub>R and Cav1 and that the affinity between

Cav1 and  $G\alpha_q(\text{GDP})$  is not sufficiently high to displace endogenous proteins from Cav1.

## DISCUSSION

In this study, we have determined the influence of caveolae on the properties of two GPCRs. The impetus for this work grew out of observations that certain signaling proteins, such as  $G\alpha_q$ , partition into caveolae domains and this partitioning alters the properties of  $G\alpha_q$ -generated signals (e.g., ref 31). Because many GPCRs that are coupled to  $G\alpha_i$  as well as  $G\alpha_q$  have been reported to reside in caveolae, we wanted to determine the influence of this domain on GPCR signaling. We used fluorescence measurements on intact living cells to avoid some of the problems in interpreting results using methods that involve cell disruption. It is arguable that the fluorescent labels used in live cell studies may influence our results. However, the subcellular localization of these proteins and functional studies argue against this possibility.

We first found that Cav1, and presumably caveolae, are not evenly distributed in FRT cells. It is important to note that the localization of caveolae may differ depending on a variety of factors, including the cell type, the confluency,<sup>32</sup> the migration state,<sup>33</sup> or its stage in the mitotic cycle.<sup>34</sup> In FRTcav+ cells, we observe Cav1 mainly on the basolateral membrane and in areas of cell–cell contact, supporting the idea that they may play a role in sensing contact inhibition or cell communication by organizing proteins such as connexins.<sup>32,35,36</sup> It is notable that in muscle tissue in which cells are arranged in arrays, such as cardiomyocytes, caveolae have a dense and fairly uniform membrane distribution along actin lines (e.g., refs 17 and 37). In fluid cells, transformed cells, or immortalized cells, caveolae are absent or their level is greatly diminished.<sup>38,39</sup> We also observed that the basolateral distribution of  $B_2R$  mirrors that of Cav1 in these cells while the distribution of  $\mu\text{OR}$  does not.

We studied the effect of caveolae on the functional and physical properties of two types of GPCRs,  $B_2R$  and  $\mu\text{OR}$ , which have both been found to localize in caveolae domains.<sup>13,40–43</sup>  $\mu\text{OR}$  and  $B_2R$  are coupled to two different families of G-proteins,  $G\alpha_i$  and  $G\alpha_q$ , respectively. Cav1 expression does not appear to affect cAMP signals generated through  $\mu\text{OR}$  and  $G\alpha_i$ . It is noteworthy that stimulation of the  $\mu\text{OR}-G\alpha_i$  pathway may also increase the level of intracellular  $\text{Ca}^{2+}$ , possibly through coactivation of a  $G\alpha_q$ -coupled receptor or by the release of  $G\beta\gamma$  subunits that can then activate  $\text{PLC}\beta_2$  or  $\text{PLC}\beta_3$ .<sup>44</sup> However, in our hands, FRTwt and FRTcav+ cells expressing  $\mu\text{OR}$  did not exhibit intracellular  $\text{Ca}^{2+}$  release. In contrast,  $\text{Ca}^{2+}$  signaling through the  $B_2R$  pathways is clearly affected by the presence of caveolae as seen in both single-cell and cell suspension measurements similar to the behavior seen for muscarinic receptors.<sup>16</sup> It is important to note that the effect of caveolae on  $\text{Ca}^{2+}$  release is seen immediately after stimulation and before detachment of  $B_2R$  from  $G\alpha_q$  and the subsequent sequestration because  $G\alpha_q-B_2R$  FRET is constant for the first 2 min after stimulation. This effect of caveolae on  $\text{Ca}^{2+}$  signals is interpreted to be due to stabilization of the activated state of  $G\alpha_q$  by strong Cav1 binding and release of  $G\beta\gamma$  from caveolae domains, which lengthens the time for recombination of the heterotrimer.<sup>16</sup> These studies and our findings presented here suggest that both  $B_2R$  and muscarinic receptors may reside in or close to caveolae.

We find both receptors colocalize with Cav1. It is notable that Head and co-workers found that  $\mu\text{OR}$  and Cav3 colocalize to a higher degree in adult cardiomyocytes,<sup>13</sup> although direct

comparison between their studies and ours is difficult because Cav3 shows a much higher level of expression and is uniformly distributed throughout cardiomyocytes as opposed to FRT cells. Additionally, the C-terminus of Cav3 is significantly different from Cav1, which may allow direct or indirect  $\mu\text{OR}$  binding. It is notable that the resolution of colocalization measurements is quite low compared to that of FRET, and we could not detect a significant amount of FRET between  $\mu\text{OR}$  and Cav1 but did find a small ( $\sim 20\%$ ) amount FRET between  $B_2R$  and Cav1. Additionally, we observed a larger amount of FRET between  $G\alpha_q$  and Cav1, implying that  $G\alpha_q$  is localized within caveolae domains. We also observe an equally large amount of FRET between  $G\alpha_q$  and  $B_2R$  (Figure 3 and ref 15). Together with our functional results, these data show that  $G\alpha_q$  can interact with Cav1 and change its signaling properties while being in the proximity of  $B_2R$ . The lower level of FRET observed between  $B_2R$  and Cav1 compared to that between  $G\alpha_q$  and Cav1 might be correlated to a weaker interaction, although it could also be traced to orientations of eCFP and eYFP that make transfer less favorable.

Our data show that Cav1 stabilizes  $G\alpha_q$ -mediated  $\text{Ca}^{2+}$  signals generated through bradykinin in  $B_2R$ -transfected cells. This receptor population is large enough to undergo FRET with Cav1 on the nanosecond time scale and to influence  $G\alpha_q$  signaling. The level of  $G\alpha_q$ -Cav1 FRET is 2-fold higher than the level of  $B_2R$ -Cav1 FRET, despite the high FRET values between  $B_2R$  and  $G\alpha_q$ . One explanation of this result is that GPCRs do not significantly penetrate into Cav1 domains and their association depends on the strength of their attached  $G\alpha$  family.  $G\alpha_q$ , which interacts strongly with Cav1, promotes caveolae localization of its coupled receptors, while  $G\alpha_i$ -coupled receptors, such as  $\mu\text{OR}$ , have little interaction with these domains, although they might incorporate into non-caveolae cholesterol-rich domains. Our fluorescence and functional studies suggest that the interaction between  $B_2R$  and Cav1 could be mediated through  $G\alpha_q$ . We find a loss of  $B_2R$ -Cav1 FRET when  $G\alpha_q$  is downregulated or displaced from caveolae, and we find that  $G\alpha_q$  but not  $G\alpha_i$  increases the level of FRET between  $B_2R$  and Cav1. These results also suggest that GPCRs that do not couple to  $G\alpha_q$ , such as  $\mu\text{OR}$  would not localize to caveolae with the overexpression of  $G\alpha_q$ . The idea that G-proteins mediate receptor association with caveolae is also supported by observations that  $\mu\text{OR}$  and  $B_2R$  can be preassembled with their G-protein subunits, and that  $G\alpha_q$ , but not other G-proteins, interacts with Cav1.<sup>12,45</sup> Additionally, previous FRET studies suggest that  $G\alpha_q$  can interact simultaneously with  $G\beta\gamma$ ,  $B_2R$ , and Cav1.<sup>15,16</sup>

Even though FRT cells have been used extensively to study caveolae, we tested the effects of caveolae on  $\text{Ca}^{2+}$  signals mediated through bradykinin in A10 cells that endogenously express  $B_2R$  and Cav1. Single-cell measurements show two distinct  $\text{Ca}^{2+}$  responses that we interpret to be due to caveolae and non-caveole localized  $G\alpha_q$ . The basis for these two populations is uncertain. It is possible that only  $\sim 30\%$  of A10 cells have fully formed caveolae domains where  $G\alpha_q$  can properly localize and impact the signaling. On the basis of the localization of caveolae on plasma membranes, we suggest that the caveolae-localized  $G\alpha_q$  population is in regions of cell–cell contact. This idea leads to the hypothesis that signaling in intercellular regions differs from that in other regions of the cell.

It is possible that instead of stabilizing the activated state of  $G\alpha_q$ , Cav1 mediates a step downstream of  $G\alpha_q$  that is coupled

to B<sub>2</sub>R and to muscarinic receptors. We have previously found that PLC $\beta$  associates strongly in a manner similar to that of G $\alpha_q$  in FRTwt and FRTcav+ cells, and because the activity of PLC $\beta$  is low in the basal state, its activity mirrors the activation state of G $\alpha_q$ , which has been observed to be prolonged in the presence of caveolae.<sup>17</sup> It is also possible that specific partitioning of PIP<sub>2</sub> in caveolae contributes to the observed changes in Ca<sup>2+</sup> release, although preferential localization of PIP<sub>2</sub> in caveolae domains is controversial (see ref 46). Interestingly, PIP<sub>2</sub> was shown to localize to the periphery of caveolae,<sup>47</sup> where we suggest that G $\alpha_q$  receptors localize. Partitioning of PIP<sub>2</sub> in the neck of caveolae would be expected to impact the magnitude of calcium release, which we see in FRTcav+ cells when they are stimulated with bradykinin, but we find that caveolae impact the duration of the signal rather than the extent<sup>16</sup> (Figures 2b and 3).

Support for the idea that GPCRs coupled to G $\alpha_q$  interact more extensively with caveolae than receptors coupled to other G-protein families comes from several reports. Many receptors that are reported to be localized and/or internalized via caveolae are coupled to G $\alpha_q$  (i.e., B<sub>2</sub>R,<sup>41,48–50</sup> endothelin Etb,<sup>51,52</sup> GnRH,<sup>53,54</sup> serotonin 5HT<sub>2</sub>,<sup>55</sup> TRH,<sup>56</sup> and muscarinic receptor M3<sup>57</sup>). With the exception of somatostatin SST<sub>2</sub>,<sup>58,59</sup> which was shown by electron microscopy to go to caveolae domains upon agonist stimulation, the two G $\alpha_q$ -coupled GPCRs that have been reported to be in caveolae have been studied using methods that require cellular disruption (sphingosine EDG-1<sup>60</sup> and muscarinic M2<sup>61,62</sup>). Additionally, these receptors may be coupled to G $\alpha_q$  as well as G $\alpha_i$  and form heterodimers with G $\alpha_q$ -coupled GPCRs. It is also notable that disruption of caveolae domains by methyl- $\beta$ -cyclodextrin attenuated the Ca<sup>2+</sup> response of the G $\alpha_q$ -coupled SHTA receptor but did not affect the release of Ca<sup>2+</sup> from the G $\alpha_q$ -coupled  $\alpha$ 1-adrenergic receptor.<sup>55</sup> However, it is possible that methyl- $\beta$ -cyclodextrin treatment does not completely disrupt the strong Cav1–G $\alpha_q$  association that results in dissociation of G $\beta\gamma$  subunits resulting in prolonged Ca<sup>2+</sup> signals.

Localization of signaling proteins in caveolae would be expected to impact their signaling properties if this sequestration prevented or promoted access to proteins in their pathway. The studies here suggest that caveolae may impact G $\alpha_q$  signaling without a direct incorporation of GPCRs into the domain. This idea might explain many of the controversial reports pertaining to GPCR–caveolae associations. Super-resolution studies will aim to improve our understanding of the organization of these domains.

## AUTHOR INFORMATION

### Corresponding Author

\*Department Physiology and Biophysics, Stony Brook University, Stony Brook, NY 11794-8661. Phone: (631) 444-3071. E-mail: suzanne.scarlata@stonybrook.edu.

### Funding

This work was supported by National Institutes of Health Grant GM053132.

### Notes

The authors declare no competing financial interest.

## ACKNOWLEDGMENTS

We thank Drs. Deborah Brown, Yuanjian Guo, Urszula Golebiewska, and Finly Philip for their helpful comments throughout this work.

## ABBREVIATIONS

A10 cells, rat aortic smooth muscle cells; B<sub>2</sub>R, bradykinin type 2 receptor; Cav1, caveolin-1; eGFP, eCFP, and eYFP, enhanced green, cyano, and yellow fluorescent proteins, respectively; FRET, Förster resonance energy transfer; FRT cells, Fischer rat thyroid cells; GPCR, G-protein-coupled receptor;  $\mu$ OR,  $\mu$ -opioid receptor; PIP<sub>2</sub>, phosphoinositol 4,5-bisphosphate; PLC $\beta$ , inositol specific mammalian phospholipase C $\beta$ .

## REFERENCES

- (1) Anderson, R. G. (1998) The caveolae membrane system. *Annu. Rev. Biochem.* 67, 199–225.
- (2) Schlegel, A., Volonte, D., Engelman, J. A., Galbiata, F., Mehta, P., Zhange, X.-L., Scherer, P., and Lisanti, M. P. (1998) Crowded little caves: Structure and function of caveolae. *Cell. Signalling* 10, 457–463.
- (3) Stan, R. V. (2005) Structure of caveolae. *Biochim. Biophys. Acta* 1746, 334–348.
- (4) Navarro, A., Anand-Apte, B., and Parat, M.-O. (2004) A role for caveolae in cell migration. *FASEB J.* 18, 1801–1811.
- (5) Okamoto, T., Schlegel, A., Scherer, P. E., and Lisanti, M. P. (1998) Caveolins, a family of scaffolding proteins for organizing “preassembled signaling complexes” at the plasma membrane. *J. Biol. Chem.* 273, 5419–5422.
- (6) Ostrom, R. S., and Insel, P. (2004) The evolving role of lipid rafts and caveolae in G protein-coupled receptor signaling: Implications for molecular pharmacology. *Br. J. Pharmacol.* 143, 235–245.
- (7) Parton, R. G., and Simons, K. (2007) The multiple faces of caveolae. *Nat. Rev. Mol. Cell Biol.* 8, 185–194.
- (8) Rybin, V. O., Xu, X., Lisanti, M. P., and Steinberg, S. F. (2000) Differential targeting of  $\beta$ -adrenergic receptor subtypes and adenylyl cyclase to cardiomyocyte caveolae. A mechanism to functionally regulate the cAMP signaling pathway. *J. Biol. Chem.* 275, 41447–41457.
- (9) Brown, D. A., and London, E. (1998) Functions of lipid rafts in biological membranes. *Annu. Rev. Cell Dev. Biol.* 14, 111–136.
- (10) Chini, B., and Parenti, M. (2004) G-protein coupled receptors in lipid rafts and caveolae: How, when and why do they go there? *J. Mol. Endocrinol.* 32, 325–338.
- (11) Alberts, B., Bray, D., Lewis, J., Raff, M., Roberts, K., and Watson, J. (1994) *Molecular Biology of the Cell*, Garland, New York.
- (12) Oh, P., and Schnitzer, J. E. (2001) Segregation of heterotrimeric G proteins in cell surface microdomains. G<sub>q</sub> binds caveolin to concentrate in caveolae, whereas G<sub>i</sub> and G<sub>s</sub> target lipid rafts by default. *Mol. Biol. Cell* 12, 685–698.
- (13) Head, B. P., Patel, H. H., Roth, D. M., Lai, N. C., Niesman, I. R., Farquhar, M. G., and Insel, P. A. (2005) G-protein-coupled Receptor Signaling Components Localize in Both Sarcolemmal and Intracellular Caveolin-3-associated Microdomains in Adult Cardiac Myocytes. *J. Biol. Chem.* 280, 31036–31044.
- (14) Dowal, L., Provitera, P., and Scarlata, S. (2006) Stable association between G $\alpha_q$  and phospholipase C $\beta$ 1 in living cells. *J. Biol. Chem.* 281, 23999–24014.
- (15) Philip, F., Sengupta, P., and Scarlata, S. (2007) Signaling through a G protein coupled receptor and its corresponding G protein follows a stoichiometrically limited model. *J. Biol. Chem.* 282, 19203–19216.
- (16) Sengupta, P., Philip, F., and Scarlata, S. (2008) Caveolin-1 alters Ca<sup>2+</sup> signal duration through specific interaction with the G $\alpha_q$  family of G proteins. *J. Cell Sci.* 121, 1363–1372.
- (17) Guo, Y., Golebiewska, U., and Scarlata, S. (2011) Modulation of Ca<sup>2+</sup> Activity in Cardiomyocytes through Caveolae-G $\alpha_q$  Interactions. *Biophys. J.* 100, 1599–1607.
- (18) Lipardi, C., Mora, R., Colomer, V., Paladino, S., Nitsch, L., Rodriguez-Boulant, E., and Zurzolo, C. (1998) Caveolin transfection results in caveolae formation but not apical sorting of glycosylphosphatidylinositol (GPI)-anchored proteins in epithelial cells. *J. Cell Biol.* 140, 617–626.

- (19) Mora, R., Bonilha, V. L., Marmorstein, A., Scherer, P. E., Brown, D., Lisanti, M. P., and Rodriguez-Boulan, E. (1999) Caveolin-2 localizes to the Golgi complex but redistributes to plasma membrane, caveolae, and rafts when co-expressed with caveolin-1. *J. Biol. Chem.* 274, 25708–25717.
- (20) Law, P.-Y., Wong, Y. H., and Loh, H. H. (2000) Molecular Mechanisms and Regulation of Opioid Receptor Signaling. *Annu. Rev. Pharmacol. Toxicol.* 40, 389–430.
- (21) Berg, K. A., Zardeneta, G., Hargreaves, K. M., Clarke, W. P., and Milam, S. B. (2007) Integrins regulate opioid receptor signaling in trigeminal ganglion neurons. *Neuroscience* 144, 889–897.
- (22) Zhao, H., Loh, H. H., and Law, P. Y. (2006) Adenylyl Cyclase Superactivation Induced by Long-Term Treatment with Opioid Agonist Is Dependent on Receptor Localized within Lipid Rafts and Is Independent of Receptor Internalization. *Mol. Pharmacol.* 69, 1421–1432.
- (23) Gaudreault, S. B., Blain, J.-F., Gratton, J.-P., and Poirier, J. (2005) A role for caveolin-1 in post-injury reactive neuronal plasticity. *J. Neurochem.* 92, 831–839.
- (24) Kang, M. J., Chung, Y. H., Hwang, C., Murata, M., Fujimoto, T., Mook-Jung, I. H., Cha, C. I., and Park, W.-Y. (2006) Caveolin-1 upregulation in senescent neurons alters amyloid precursor protein processing. *Exp. Mol. Med.* 38, 126–133.
- (25) Yu, C., Rouen, S., and Dobrowsky, R. T. (2008) Hyperglycemia and downregulation of caveolin-1 enhance neuregulin-induced demyelination. *Glia* 56, 877–887.
- (26) Faussner, A., Bathon, J. M., and Proud, D. (1999) Comparison of the responses of B1 and B2 kinin receptors to agonist stimulation. *Immunopharmacology* 45, 13–20.
- (27) Narayanan, V., Guo, Y., and Scarlata, S. (2005) Fluorescence studies suggest a role for  $\alpha$ -synuclein in the phosphatidylinositol lipid signaling pathway. *Biochemistry* 44, 462–470.
- (28) Runnels, L. W., and Scarlata, S. F. (1999) Determination of the Affinities between Heterotrimeric G Protein Subunits and Their Phospholipase C- $\beta$  Effectors. *Biochemistry* 38, 1488–1496.
- (29) Chen, Y., Elangovan, M., and Periasamy, A. (2005) FRET Data Analysis: The Algorithm. In *Molecular Imaging: FRET Microscopy and Spectroscopy* (Day, P. A., Ed.) Chapter 7, Oxford University Press, New York.
- (30) Golebiewska, U., Johnston, J. M., Devi, L., Filizola, M., and Scarlata, S. (2011) Differential Response to Morphine of the Oligomeric State of  $\mu$ -Opioid in the Presence of  $\delta$ -Opioid Receptors. *Biochemistry* 50, 2829–2837.
- (31) Golebiewska, U., and Scarlata, S. (2010) The effect of membrane domains on the G protein–phospholipase C $\beta$  signaling pathway. *Crit. Rev. Biochem. Mol. Biol.* 45, 97–105.
- (32) Volontè, D., Galbiati, F., and Lisanti, M. P. (1999) Visualization of caveolin-1, a caveolar marker protein, in living cells using green fluorescent protein (GFP) chimeras: The subcellular distribution of caveolin-1 is modulated by cell-cell contact. *FEBS Lett.* 445, 431–439.
- (33) Isshiki, M., Ando, J., Yamamoto, K., Fujita, T., Ying, Y., and Anderson, R. G. W. (2002) Sites of Ca<sup>2+</sup> wave initiation move with caveolae to the trailing edge of migrating cells. *J. Cell Sci.* 115, 475–484.
- (34) Boucrot, E., Howes, M. T., Kirchhausen, T., and Parton, R. G. (2011) Redistribution of caveolae during mitosis. *J. Cell Sci.* 124, 1965–1972.
- (35) Schubert, A.-L., Schubert, W., Spray, D. C., and Lisanti, M. P. (2002) Connexin Family Members Target to Lipid Raft Domains and Interact with Caveolin-1. *Biochemistry* 41, 5754–5764.
- (36) Langlois, S., Cowan, K. N., Shao, Q., Cowan, B. J., and Laird, D. W. (2008) Caveolin-1 and -2 Interact with Connexin43 and Regulate Gap Junctional Intercellular Communication in Keratinocytes. *Mol. Biol. Cell* 19, 912–928.
- (37) Woodman, S. E., Park, D. S., Cohen, A. W., Cheung, M. W.-C., Chandra, M., Shirani, J., Tang, B., Jelicks, L. A., Kitsis, R. N., Christ, G. J., Factor, S. M., Tanowitz, H. B., and Lisanti, M. P. (2002) Caveolin-3 Knock-out Mice Develop a Progressive Cardiomyopathy and Show Hyperactivation of the p42/44 MAPK Cascade. *J. Biol. Chem.* 277, 38988–38997.
- (38) Koleske, A. J., Baltimore, D., and Lisanti, M. P. (1995) Reduction of caveolin and caveolae in oncogenically transformed cells. *Proc. Natl. Acad. Sci. U.S.A.* 92, 1381–1385.
- (39) Engelman, J. A., Wykoff, C. C., Yasuhara, S., Song, K. S., Okamoto, T., and Lisanti, M. P. (1997) Recombinant Expression of Caveolin-1 in Oncogenically Transformed Cells Abrogates Anchorage-independent Growth. *J. Biol. Chem.* 272, 16374–16381.
- (40) Lamb, M., Zhang, C., Shea, T., Kyle, D., and Leeb-Lundberg, L. M. F. (2002) Human B1 and B2 bradykinin receptors and their agonists target caveolae-related lipid rafts to different degrees in HEK293 cells. *Biochemistry* 41, 14340–14347.
- (41) de Weerd, W. F. C., and Leeb-Lundberg, L. M. F. (1997) Bradykinin Sequesters B2 Bradykinin Receptors and the Receptor-coupled G $\alpha$  Subunits G $\alpha$ q and G $\alpha$ iin Caveolae in DDT1MF-2 Smooth Muscle Cells. *J. Biol. Chem.* 272, 17858–17866.
- (42) Haasemann, M., Cartaud, J., Muller-Esterl, W., and Dunia, I. (1998) Agonist-induced redistribution of bradykinin B2 receptor in caveolae. *J. Cell Sci.* 111 (Part 7), 917–928.
- (43) Zheng, H., Chu, J., Qiu, Y., Loh, H. H., and Law, P.-Y. (2008) Agonist-selective signaling is determined by the receptor location within the membrane domains. *Proc. Natl. Acad. Sci. U.S.A.* 105, 9421–9426.
- (44) Philip, F., Kadamur, G., Silos, R. G., Woodson, J., and Ross, E. M. (2010) Synergistic Activation of Phospholipase C- $\beta$ 3 by G $\alpha$ q and G $\beta$ 3 Describes a Simple Two-State Coincidence Detector. *Curr. Biol.* 20, 1327–1335.
- (45) Murthy, K. S., and Makhlof, G. M. (2000) Heterologous desensitization mediated by G protein-specific binding to caveolin. *J. Biol. Chem.* 275 (39), 30211–30219.
- (46) Morris, J. B., Huynh, H., Vasilevski, O., and Woodcock, E. A. (2006)  $\alpha$ 1-Adrenergic receptor signaling is localized to caveolae in neonatal rat cardiomyocytes. *J. Mol. Cell. Cardiol.* 41, 17–25.
- (47) Fujita, A., Cheng, J., Tauchi-Sato, K., Takenawa, T., and Fujimoto, T. (2009) A distinct pool of phosphatidylinositol 4,5-bisphosphate in caveolae revealed by a nanoscale labeling technique. *Proc. Natl. Acad. Sci. U.S.A.* 106, 9256–9261.
- (48) Haasemann, M., Cartaud, J., Muller-Esterl, W., and Dunia, I. (1998) Agonist-induced redistribution of bradykinin B2 receptor in caveolae. *J. Cell Sci.* 111, 917–928.
- (49) Ju, H., Venema, V. J., Liang, H., Harris, M. B., Zou, R., and Venema, R. C. (2000) Bradykinin activates the Janus-activated kinase/signal transducers and activators of transcription (JAK/STAT) pathway in vascular endothelial cells: Localization of JAK/STAT signalling proteins in plasmalemmal caveolae. *Biochem. J.* 351, 257–264.
- (50) Lamb, M. E., Zhang, C., Shea, T., Kyle, D. J., and Leeb-Lundberg, L. M. F. (2002) Human B1 and B2 Bradykinin Receptors and Their Agonists Target Caveolae-Related Lipid Rafts to Different Degrees in HEK293 Cells. *Biochemistry* 41, 14340–14347.
- (51) Teixeira, A., Chaverot, N., Schröder, C., Strosberg, A. D., Couraud, P.-O., and Cazaubon, S. (1999) Requirement of Caveolae Microdomains in Extracellular Signal-Regulated Kinase and Focal Adhesion Kinase Activation Induced by Endothelin-1 in Primary Astrocytes. *J. Neurochem.* 72, 120–128.
- (52) Yamaguchi, T., Murata, Y., Fujiyoshi, Y., and Doi, T. (2003) Regulated interaction of endothelin B receptor with caveolin-1. *Eur. J. Biochem.* 270, 1816–1827.
- (53) Navratil, A. M., Bliss, S. P., Berghorn, K. A., Haughian, J. M., Farmerie, T. A., Graham, J. K., Clay, C. M., and Roberson, M. S. (2003) Constitutive Localization of the Gonadotropin-releasing Hormone (GnRH) Receptor to Low Density Membrane Microdomains Is Necessary for GnRH Signaling to ERK. *J. Biol. Chem.* 278, 31593–31602.
- (54) Pawson, A. J., Maudsley, S. R., Lopes, J., Katz, A. A., Sun, Y.-M., Davidson, J. S., and Millar, R. P. (2003) Multiple Determinants for Rapid Agonist-Induced Internalization of a Nonmammalian Gonadotropin-Releasing Hormone Receptor: A Putative Palmitoylation Site

and Threonine Doublet within the Carboxyl-Terminal Tail Are Critical. *Endocrinology* 144, 3860–3871.

(55) Dreja, K., Voldstedlund, M., Vinten, J., Tranum-Jensen, J., Hellstrand, P., and Sward, K. (2002) Cholesterol Depletion Disrupts Caveolae and Differentially Impairs Agonist-Induced Arterial Contraction. *Arterioscler., Thromb., Vasc. Biol.* 22, 1267–1272.

(56) Drmota, T., Novotny, J., Gould, G. W., Svoboda, P., and Milligan, G. (1999) Visualization of distinct patterns of subcellular redistribution of the thyrotropin-releasing hormone receptor-1 and Gq $\alpha$ /G11 $\alpha$  induced by agonist stimulation. *Biochem. J.* 340, 529–538.

(57) Gosens, R., Stelmack, G. L., Dueck, G., Mutawe, M. M., Hinton, M., McNeill, K. D., Paulson, A., Dakshinamurti, S., Gerthoffer, W. T., Thliveris, J. A., Unruh, H., Zaagsma, J., and Halayko, A. J. (2007) Caveolae facilitate muscarinic receptor-mediated intracellular Ca<sup>2+</sup> mobilization and contraction in airway smooth muscle. *Am. J. Physiol.* 293, L1406–L1418.

(58) Krisch, B., Feindt, J., and Mentlein, R. (1998) Immunoelectronmicroscopic Analysis of the Ligand-induced Internalization of the Somatostatin Receptor Subtype 2 in Cultured Human Glioma Cells. *J. Histochem. Cytochem.* 46, 1233–1242.

(59) Mentlein, R., Held-Feindt, J., and Krisch, B. (2001) Topology of the signal transduction of the G protein-coupled somatostatin receptor sst<sub>2</sub> in human glioma cells. *Cell Tissue Res.* 303, 27–34.

(60) Igarashi, J., and Michel, T. (2000) Agonist-modulated Targeting of the EDG-1 Receptor to Plasmalemmal Caveolae. *J. Biol. Chem.* 275, 32363–32370.

(61) Feron, O., Smith, T. W., Michel, T., and Kelly, R. A. (1997) Dynamic Targeting of the Agonist-stimulated m2Muscarinic Acetylcholine Receptor to Caveolae in Cardiac Myocytes. *J. Biol. Chem.* 272, 17744–17748.

(62) Dessy, C., Kelly, R. A., Balligand, J.-L., and Feron, O. (2000) Dynamin mediates caveolar sequestration of muscarinic cholinergic receptors and alteration in NO signaling. *EMBO J.* 19, 4272–4280.